

## Studying the Thermal Influence on the Vibration of Rotating Blades

Abbas Fadhil Abbas<sup>1,\*</sup>, Adawiya Ali Hamzah<sup>2</sup>

<sup>1</sup>*Aeronautical Eng. Technologies Dept., Technical College of Engineering, Al-Farahidi University, Baghdad, Iraq, [abbas.f.alzubaidi@uoalfarahidi.edu.iq](mailto:abbas.f.alzubaidi@uoalfarahidi.edu.iq)*

<sup>2</sup>*Department of Energy Engineering, University of Baghdad, Baghdad, Iraq*

Computing the vibrating characteristics of any machine or structure is a necessary process that should be performed by the mechanical engineers that work in engineering design field to avoid the collapse under different kinds of applied loads. One of these kinds of structures are the rotating blades, whereas this part is considered as an essential element in many rotating systems that are used in different fields of engineering, e.g., turbomachinery, turbofan, helicopters, etc. One of the biggest disadvantages that is realized in rotating blades is failure due to vibrations and unbalance. It is possible that vibrations significantly reduce the performance of rotating blades compared to standard design conditions. If these rotating blades continue to operate under these circumstances for sufficient time, then the status of these systems will be unstable. Finally, this will lead to collapse of the rotating blades. In this work, a new code was created from scratch, based on the finite element method, to determine the vibrational characteristics of the rotating blades, taking into consideration the effect of rotating speed and temperatures. The compound influence of thermal gradients and rotating speed on the vibrational response (frequencies) for different configurations of blade was studied deeply.

Keywords: Vibration analysis, FE method; rotating blade; thermal effect.

### 1. INTRODUCTION

In many engineering systems, the rotating blades are a necessary element to accomplish the desirable process. There is a wide range of scales for rotating blades, where it starts from small scale to the large one. The main concept to obtain the successful systems that contain rotating blades is the stability, where these systems should work within the stability zone, especially under the high rotating speed. The main factors affecting significantly the stability of many systems are the vibration and the high thermal gradients. The typical geometry of rectangular rotating blade can be seen in Fig. 1.

Due to the rapid development in the industrial sector, we focus particularly on the dynamic analysis (vibration), and the topic of thermal effect (high change in temperature) on the vibration of the structures (e.g., rotating blades). This problem has become an essential matter to the design engineers. Therefore, the researches focus to study deeply the factors affecting the vibration characteristics of the rotating blades. It can be considered that one of the main points to obtain a successful design for any machine element or structure is the accurate computation of the dynamic behavior of the selected machine element or system.

Also, there are other important factors that have direct effect on the dynamical response of the rotating blades (or any other structure), which are the material properties of the structure

itself, constraints conditions, geometry, etc., where the stiffness of any part is related directly to physical properties of the material such as the elastic modulus. If there is any change in the material properties, the magnitude of stiffness for this structure will be changed significantly. As a result of this change in structural stiffness, the vibrational behavior will change as well.

Farsadi [1] investigated the effect of variable stiffness on the dynamic behavior of the Composite pre-twisted tapered rotating beam (thin-wall). Such rotating blades are used in different applications such as wind turbine, fans, helicopters, and turbomachinery. He focused in his research on the effect of the critical buckling load on the frequencies of the blades. He enhanced the analytical solution in addition to applying the numerical software (ABAQUS) for providing significant data for designers to fill the gap about the effect of the variable stiffness on the rotating blades.

Ruan and Hajek [2] studied numerically a single pitching rotating blade taking into consideration the influence of the flow. They assumed that there is edge vortex, including tip vortex and they found that the swell structure affects significantly the response of the system. They suggested building a mathematical model of the dynamic problem of the rotating blade, it is better to assume 3D vortex included in the blade element momentum approach in order to obtain more accurate results.

Chen and Li [3] developed a theoretical approach to study the dynamic behavior of the pre-twisted rotating composite laminated blade based on shell theory. In their model, they took the influences of the centrifugal Coriolis and forces into consideration in order to find the natural frequencies. Rafiee et al. [4] presented the previous works that covered the dynamic behavior of the rotating blades. They showed the influences of many parameters such as twist angle, aspect ratio, rotational speed, radius of the hub on the dynamic behavior of the rotation blade. It was found that the main significant factor is the rotational speed and the twist angle, while the other factors have less influence.

Yang et al. [5] studied the dynamic behavior of cracked rotating blade. They included in their model the centrifugal stiffener, Coriolis effect, and spinning softener. They developed their model based on the strain energy release rate and continuous beam theories. They verified their results with the FE solution and found that the crack and its position have great influence on the dynamic behavior of the rotating blade. The maximum effect occurred near the root and the minimum one near the tip. The cracks are related directly to the stiffness of the blade where they reduce the stiffness. Wang et al. [6] presented a mathematical model of the turbine blades based on the coupling effect of the fluid and dynamic effect (vortices and the rotational speed). They found the nonlinear response and state of stability of the rotating blades, their results presented the frequencies and mode shapes under different configurations.

Yao et al. [7] investigated the pre-twisted cylindrical rotating shell that was used in the aero-engine compressors. Also, they investigated the Coriolis force and centrifugal force on the dynamic response of the blades, in addition to the effect of the aerodynamic pressure that has significant effect on the frequencies and mode shapes. Also, they investigated the influence of damping coefficient, twist angle and fixing angle on nonlinear dynamic behavior of the blade.

Ding et al. [8] enhanced the analytical solution to find the natural frequency of the rotating ring that was fixed to an elastic foundation. Also, they applied the FE method to find the numerical solution of the same problem, where they found that the difference between the results of both approaches was not more than 5%. The rotation speed was considered in the calculation in order to find the solution of the eigenvalue problem.

There are many researchers (e.g., [9]-[12]) investigating the influence of dimensions, operating conditions, and physical properties of material on the vibration of the rotating blades in different applications. However, there are not enough researches that investigate the effect of temperature variation on the vibrational response of rotating blades, especially when this thermal effect changes quickly and with high gradient. On the other hand, there are several research papers [13]-[16] that explore the effect of cracks and speed of rotation on the dynamical response of the rotating blades.

The main objective of this paper is to compute the values of frequencies with high accuracy of the rotating blades and to know the dynamic behavior of the blade under different thermal working conditions. In order to accomplish this task, a new numerical dynamic model of the rotating blade is

presented. It was taken into account in the new numerical model of the thermal effect of the working environment on the material properties of the rotating blade (elastic modulus and Poisson's ratio), and thus affects the vibration behavior. The Fortran Language was used to simulate the vibration of the rotating blade based on new finite element code to determine the frequencies of any desired mode shapes of the rotating blade under any rotating speed and thermal conditions. The variation range for the temperature of working environment used in this research started at  $-200\text{ }^{\circ}\text{C}$  to  $200\text{ }^{\circ}\text{C}$ .

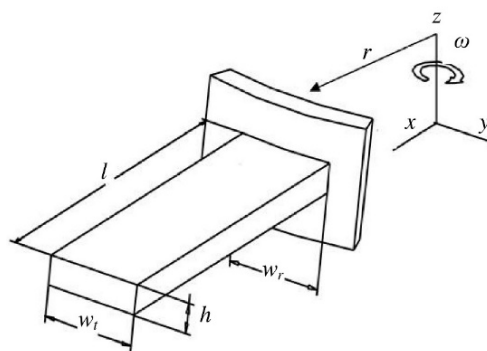


Fig.1. The geometry of rectangular rotating blade.

## 2. FORMULATIONS BASED ON FINITE ELEMENT TECHNIQUE

This section presents all necessary equations and approaches of the numerical analysis based on the Finite Element Method to obtain the modal solution of the rotating blade under thermal effect. After searching for more suitable type of element among the available ones, it was found that the shell element is the most optimal one [17]. This type of element contains four-nodes with 6-degree of freedom (DOF) for every node, where DOFs of selected element are deformations in  $x$ ,  $y$ , and  $z$  axes. Also, the rotational about  $x$ -axis and  $y$ -axis, in addition to the temperature. All details of the shell elements are described in many references (e.g., [17], [18]). In order to find the solution of the modal problem, the mass and stiffness matrices of the structure should be calculated. The displacement vector for each node of finite element model of the rotating blade in the global-coordinate is [18],

$$U = \{u, v, w\} \quad (1)$$

$\alpha$ : rotations around  $X$  axis;  $\beta$ : rotations around  $Y$  axis.

Fig.2. shows the geometry of the selected shell element, where  $Q_i$  is,

$$Q_i = \{u_i, v_i, w_i, \alpha_i, \beta_i\} \quad (i=1, \dots, 4) \quad (2)$$

Two assumptions were used to formulate the kinematics, which are: the rotations of each node are very small and nodal fiber has no ability to extend. Based on the above assumptions, we can obtain the nodal displacements as follows,

$$\begin{bmatrix} \mathbf{u} \\ \mathbf{v} \\ \mathbf{w} \end{bmatrix} = \sum_{i=1}^8 N_i \begin{bmatrix} \mathbf{u}_i \\ \mathbf{v}_i \\ \mathbf{w}_i \end{bmatrix} + \sum_{i=1}^8 N_i \zeta \frac{h_i}{2} [V_{1i} - V_{2i}] \begin{bmatrix} \alpha_i \\ \beta_i \end{bmatrix} \quad (3)$$

where  $N_i$  is shape function. The strain vector can be written as,

$$\varepsilon = \begin{bmatrix} \varepsilon_x \\ \varepsilon_y \\ \varepsilon_z \\ \gamma_{xy} \\ \gamma_{yz} \\ \gamma_{zx} \end{bmatrix} = \begin{bmatrix} u_{,x} \\ v_{,y} \\ w_{,z} \\ u_{,y} + v_{,x} \\ v_{,z} + w_{,y} \\ w_{,x} + u_{,z} \end{bmatrix} \quad (4)$$

where the stiffness matrix in the global coordinates can be written as follows,

$$[K] = \int_{vol} [B]^T [D] [B] dV \quad (5)$$

and  $B_i$  matrix is,

$$B_i = \begin{bmatrix} a_i & 0 & 0 & -d_i l_{2i} & d_i l_{1i} \\ 0 & b_i & 0 & -e_i m_{2i} & e_i m_{1i} \\ 0 & 0 & c_i & -g_i n_{2i} & g_i n_{1i} \\ b_i & a_i & 0 & -e_i l_{2i} - d_i m_{2i} & e_i l_{1i} + d_i m_{1i} \\ 0 & c_i & b_i & -g_i m_{2i} - e_i n_{2i} & g_i m_{1i} + e_i n_{1i} \\ c_i & 0 & a_i & -d_i n_{2i} - g_i l_{2i} & d_i n_{1i} + g_i l_{1i} \end{bmatrix} \quad (i=1,2,3\dots,8) \quad (6)$$

While the matrix of rigidity ( $[D]$ ) is [18],

$$[D] = \frac{E(T)h}{1-\nu(T)^2} \begin{bmatrix} 1 & \nu & 0 & 0 & 0 & 0 & 0 & 0 \\ \nu & 1 & 0 & 0 & 0 & 0 & 0 & 0 \\ 0 & 0 & \frac{1-\nu(T)}{2} & 0 & 0 & 0 & 0 & 0 \\ 0 & 0 & 0 & \frac{1-\nu(T)}{2k_1} & 0 & 0 & 0 & 0 \\ 0 & 0 & 0 & 0 & \frac{1-\nu(T)}{2k_1} & 0 & 0 & 0 \\ 0 & 0 & 0 & 0 & 0 & \frac{h^2}{12} & \frac{h^2 \nu(T)}{12} & 0 \\ 0 & 0 & 0 & 0 & 0 & \frac{h^2 \nu(T)}{12} & \frac{h^2}{12} & 0 \\ 0 & 0 & 0 & 0 & 0 & 0 & 0 & \frac{h^2(1-\nu(T))}{24} \end{bmatrix} \quad (7)$$

$\nu$ : Poisson's ratio and  $E$ : Elastic Modulus. In this analysis, the thermal effect on the rotating blade (material properties) was taken into account. The functions for Elastic Modulus and Poisson's ratio can be written as follows:

$$E = f(T) \quad (8)$$

$$\nu = f(T) \quad (9)$$

Then, the mass matrix in the global coordinates is [18],

$$[M] = \int_V \rho [N]^T [N] dV \quad (10)$$

The general equation to obtain the frequency and mode shape of the rotating blade is [19],

$$M_E q^{**} + C q^* + [K_E + K_G + K_R] q = \vec{F} (\Omega^2) \quad (11)$$

where,  $K_G$  is the stiffness that is the function of the initial stresses. It was assumed that the initial stresses are equal to zero as follows,

$$[K_E + K_R] q = \vec{F} (\Omega^2) \quad (12)$$

Later, it can be solved including the initial stresses, then the equation is,

$$(K_E + K_G(\sigma_0) + K_R) q = \vec{F} (\Omega^2) \quad (13)$$

Finally, the equation that can be used to find the frequencies and mode shapes neglecting the Coriolis effect can be written as:

$$[K_E + K_G(\sigma) + K_R - \omega^2 M_E] q_0 = 0 \quad (14)$$

Where, it was supposed that the vibration is harmonic. It adopted the simultaneous iteration approach to find the frequencies [20], [21].

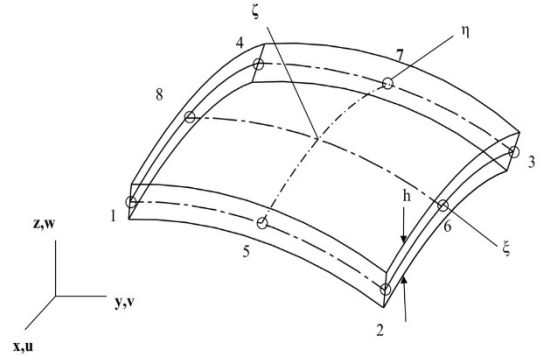


Fig.2. The geometry of the selected element (Eight nodes).

### 3. NUMERICAL ANALYSIS OF VIBRATION UNDER THERMAL EFFECT

The next important step after deriving the necessary equations in the previous section is to build a new finite element code to compute the frequencies of the rotating blade. A new general code was built using the Fortran Language to determine the dynamic characteristics under different working conditions (speed of rotation and thermal gradient) of any rotating blade. This code has the ability to calculate the frequencies of any structure under the thermal effect. A wide range of temperatures can be applied to the surrounding environment of the structure during the period of computation. All material properties of the structure are functions of the temperature of surrounding environment. In this analysis, the values of Elastic Modulus vary with temperature according to data of the selected material. New subroutine was added which is called (Auto-Mesh) to select

the suitable mesh for the rotating blade. Furthermore, the code of the subroutine (Auto-Mesh) can be modified to generate the mesh for any other structure and find the dynamic characteristics for the new case study. We can see the main steps of the new finite element program to determine the vibrational characteristics of the rotating blade in Fig.3.

The main part of code is called (MPVF), and it has the ability to achieve several tasks such as open files, read files, print the output files, etc. (MPVF) contains 4 main subroutines; (S-Data), (S-Assemb), (S-Eigen), and (S-Solver). The task of the (S-Data) is to approve the input data by (MPVF), where this subroutine contains 2 subroutines [(S-General) and (S-AutoMesh)] that are responsible for the output information. The main mission of subroutine (S-General) is defining material specifications of the rotating blade. The task of (S-AutoMesh) is generating the nodes and elements of the final mesh of the FE model of rotating blade. It can find the assembly of matrices and then determine the mass matrix and stiffness matrix by using subroutine (S-Assemb). (S-Assemb) has 4 minor subroutines; (S-Shapfun), (S-Dmatrix), (S-Jacobian), and (S-Bmatrix). It can determine the  $[B]$  matrix using the subroutine (S-Bmatrix) and the matrix of rigidities  $[D]$  using (S-Dmatrix). The task of subroutine (S-Jacobian) is to determine the Jacobian matrix, while the task of (S-Shapfun) is to find the shape function and its derivatives. The main tasks of the last two subroutines (S-Eigen) and (S-Solver) are to calculate the solutions for the Eigen-value and Eigen-vector problems. Finally, we determine the complete solutions of the system using the simultaneous iteration approach.

The first step before obtaining the results is to find the most optimal meshes for all finite element models of rotating blades in this analysis. Therefore, the convergence tests were applied to achieve this target in order to obtain the results with high precision. In this analysis, the material properties are isotropic and homogeneous. We selected the Aluminum alloys (3003, 3004 & 6063) as material for the rotating blade, where the values of density and Poisson's ratio are 2710 kg/m<sup>3</sup> and 0.33, respectively. The width of the blade is 30 mm, and disc radius is 150 mm. Fig.4. illustrates the changing of Elastic Modulus with temperature for the selected material.

Also, the accuracy of the results for the new program was checked by comparing the obtained results by using a program with the results obtained by commercial software (Ansys APDL 20) as shown in Table 1. It can be seen that the percentage difference between both results of frequencies does not exceed 1.2 %

Table 2. illustrates the comparison between present results and the results obtained by Carnegie [23] of the fundamental frequency of vibration of the steel blade. Results in Table 2. show that the maximum difference between the results obtained using different approaches did not exceed 1 %. Also, we can see the grid independence test of the rotating blade in Fig.5., in order to select the optimal mesh for the blade. Fig.6. demonstrates the finite element model of the rotating blade that was used in this analysis. The blade is fixed at the root on a disc and free to rotate with any speed.

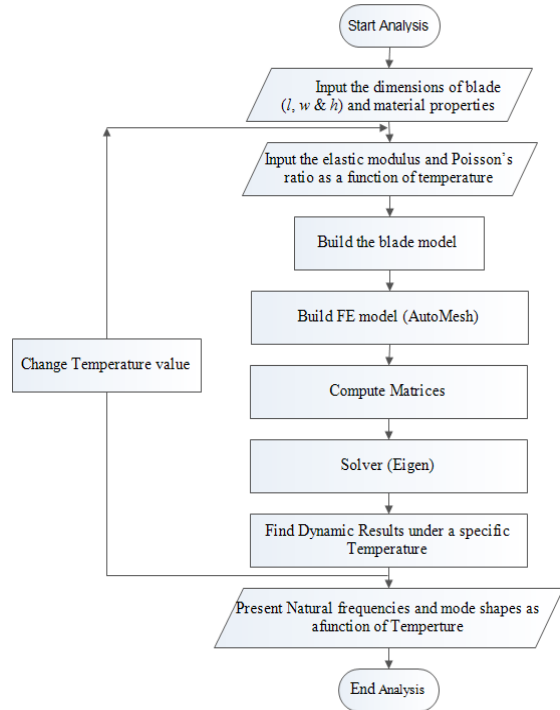


Fig.3. Schematic of developed vibrational numerical solution.

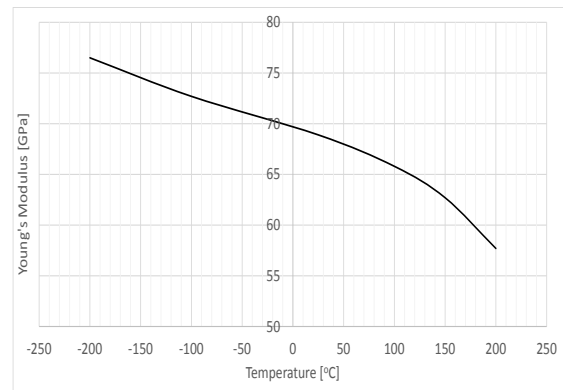


Fig.4. Changing the values of elastic modulus with temperature [22].

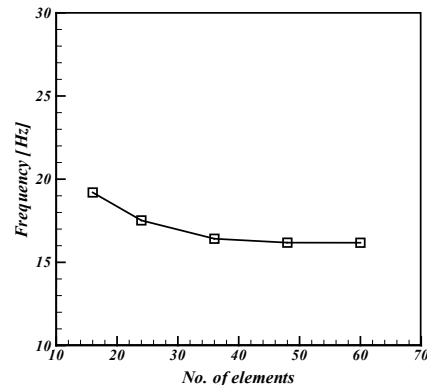


Fig.5. The grid independence test of the rotating blade (1<sup>st</sup> model,  $t = 2$  mm).

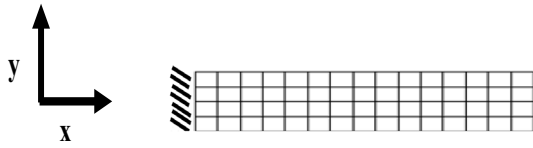


Fig.6. Finite element model of the rotating blade using the shell element.

Table 1. The fundamental frequencies of rotating blade under different rotational speed ( $t = 1$  mm).

| Rotation Speed (rad/s) | Frequency (HZ) |            | Diff. % |
|------------------------|----------------|------------|---------|
|                        | Present        | Ansys APDL |         |
| 0                      | 8.09           | 8.01       | 0.99    |
| 50                     | 11.06          | 10.95      | 1.00    |
| 100                    | 16.82          | 16.62      | 1.20    |
| 150                    | 23.13          | 22.9       | 1.00    |
| 200                    | 29.58          | 29.29      | 0.99    |

Table 2. The fundamental frequencies of rotating blade (Rotation Speed =  $100 \pi$  rad/s).

| Frequency (HZ) |           | Diff. % |
|----------------|-----------|---------|
| Present        | Ref. [23] |         |
| 52.27          | 52.75     | 0.90    |

4. RESULTS AND DISCUSSION

This research paper explored the compound effect of rotation speed and thermal influence due to the working environment on the dynamic response of the rotating blade. 3-dimensional mathematical models under different rotating speeds were built to represent the rotating blade. A new finite element program was coded using the Fortran Language to determine the frequencies accurately for different thermal gradients and rotation speed conditions. The effect of the thickness at different speeds and different surrounding temperatures on frequencies was studied deeply, where three different thicknesses were selected (1, 2, & 3 mm).

Fig.7. to Fig.9. show the effect of temperature on the first three frequencies of rotating blade under different rotating speeds using thickness 1 mm. First, we can see the significant effect of rotating speed on the values of frequencies. It can be observed that the maximum effect occurred at the highest temperature (200 °C) and rotating speed ( $\omega = 200$  rad/s), where the percentage increment in the frequencies of the 1<sup>st</sup>, 2<sup>nd</sup>, & 3<sup>rd</sup> mode were 314 %, 141 %, & 25.5 %, respectively. On the other hand, the minimum effect occurred at the lowest temperature (-200 °C) and rotating speed ( $\omega = 0$  rad/s), where the percentage increment in 1<sup>st</sup>, 2<sup>nd</sup>, & 3<sup>rd</sup> mode was 265 %, 115 %, & 25.2 %, respectively.

Fig.10. to Fig.12. illustrate the effect of temperature on the first three frequencies of the rotating blade under different rotating speeds using the blade’s thickness 2 mm. Generally, it can be noticed that the values of frequencies, when thickness is 2 mm, are higher than those of thickness equal to 1 mm. The main reason for such results is structural stiffness

of the blade increasing when the thickness of blade increases too. The same behavior of the frequencies can be seen as in the previous results, but the percentages of increments for frequencies when thickness is 2 mm are lower than those of thickness 1 mm. The percentage increment in the frequencies of the 1<sup>st</sup>, 2<sup>nd</sup>, & 3<sup>rd</sup> mode was 131 %, 49 %, & 2.5 %, when rotating speed and temperature changed from ( $\omega = 0$  rad/s,  $T = -200$  °C) to ( $\omega = 200$  rad/s,  $T = 200$  °C).

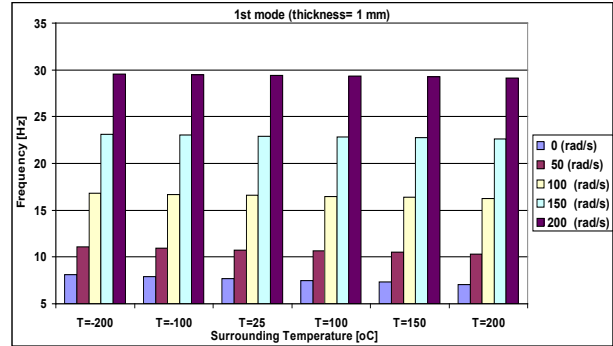


Fig.7. The variation of frequency with surrounding temperature applying different rotating speed (1<sup>st</sup> mode;  $t = 1$  mm).

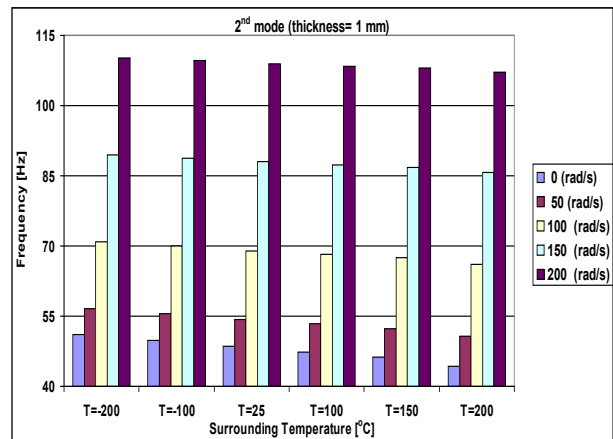


Fig.8. The variation of frequency with surrounding temperature applying different rotating speed (2<sup>nd</sup> mode;  $t = 1$  mm).

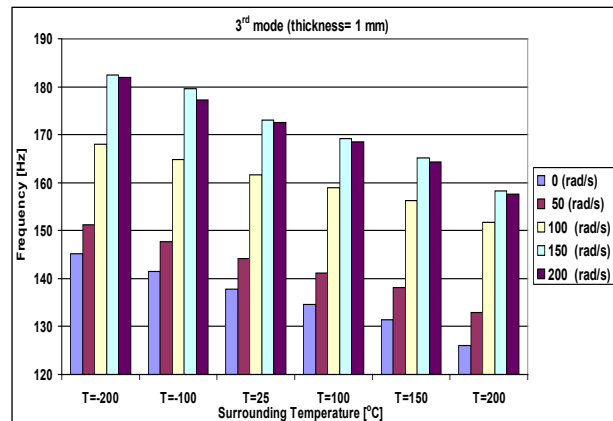


Fig.9. The variation of frequency with surrounding temperature applying different rotating speed (3<sup>rd</sup> mode;  $t = 1$  mm).

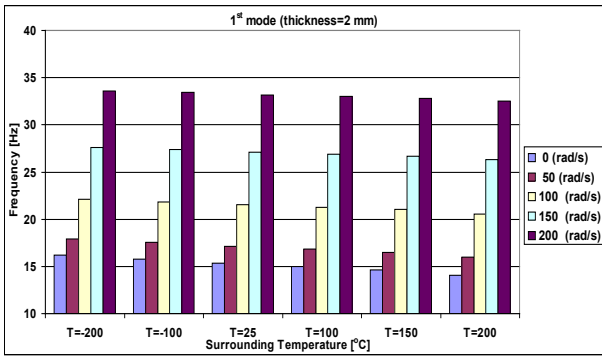


Fig.10. The variation of frequency with surrounding temperature applying different rotating speed (1<sup>st</sup> mode;  $t = 2$  mm).

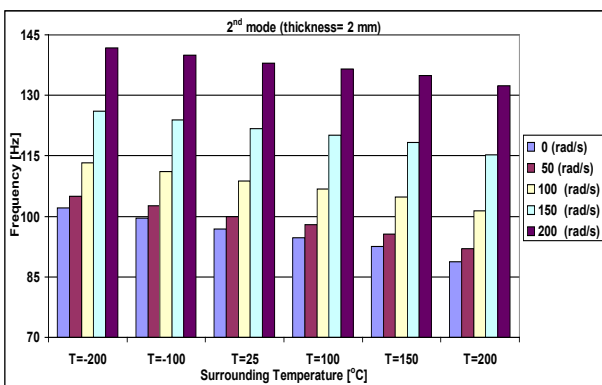


Fig.11. The variation of frequency with surrounding temperature applying different rotating speed (2<sup>nd</sup> mode;  $t = 2$  mm).

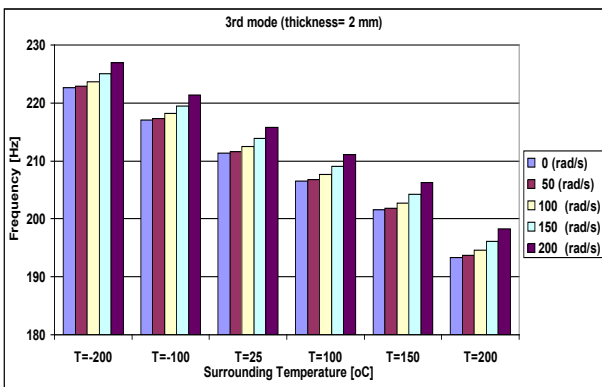


Fig.12. The variation of frequency with surrounding temperature applying different rotating speed (3<sup>rd</sup> mode;  $t = 2$  mm).

Fig.13. to Fig.15. demonstrate the effect of temperature on the first three frequencies of the rotating blade under different rotating speeds using the blade's thickness 3 mm. Also, it was noticed that the values of frequencies when thickness is 3 mm are higher than those of thicknesses 1 & 2 mm. The same behavior of the frequencies as in the previous results can be seen, but the percentages of increments for frequencies when thickness is 3 mm are lower than those of thicknesses 1 & 2 mm. The percentage increment in the frequencies of the 1<sup>st</sup>,

2<sup>nd</sup>, & 3<sup>rd</sup> mode was 73 %, 24.3 %, & 2.5 %, when rotating speed and temperature changed from ( $\omega = 0$  rad/s,  $T = -200$  °C) to ( $\omega = 200$  rad/s,  $T = 200$  °C).

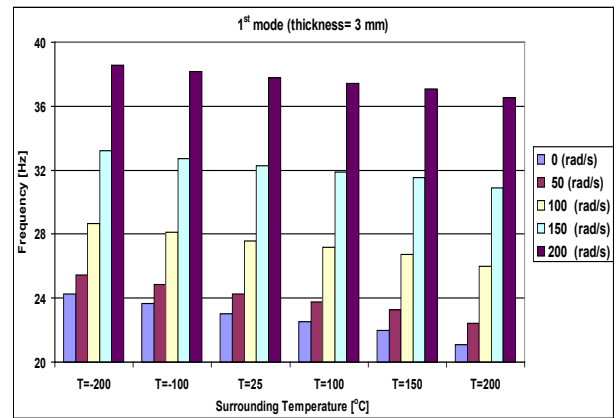


Fig.13. The variation of frequency with surrounding temperature applying different rotating speed (1<sup>st</sup> mode;  $t = 3$  mm).

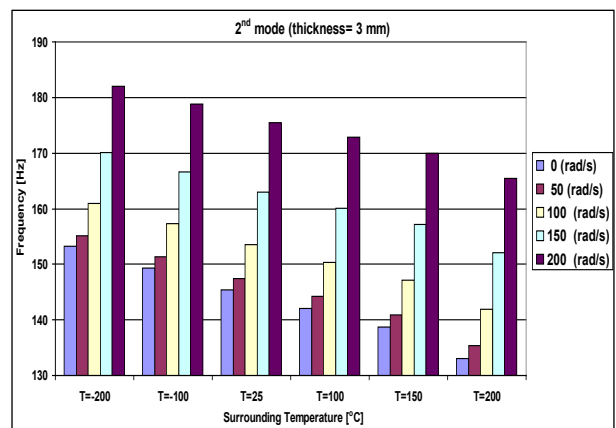


Fig.14. The variation of frequency with surrounding temperature applying different rotating speed (2<sup>nd</sup> mode;  $t = 3$  mm).

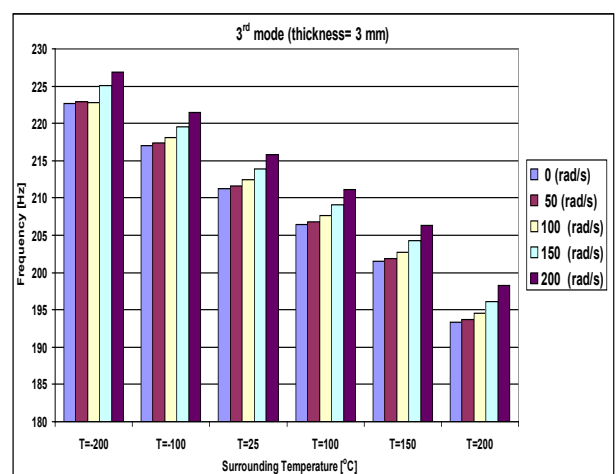


Fig.15. The variation of frequency with surrounding temperature applying different rotating speed (3<sup>rd</sup> mode;  $t = 3$  mm).

## 6. CONCLUSIONS AND REMARKS

In this work a three-dimensional numerical solution was developed based on the finite element theory to study the compound effect of high gradients of working ambient and rotating speed on the frequencies of a rotating blade. In addition we studied the effect of the blade's thickness on the magnitudes of frequencies under the influence of different surrounding temperatures and rotation speed. The new Fortran program was created and then used to obtain the numerical vibrational results. Based on the obtained results, the reliability of the new program has been proven in order to determine the frequencies of the rotating blade under different configurations and working conditions.

The main conclusion from the results is the significant influence of ambient temperatures (thermal load) on the magnitudes of frequencies for blades and the highest effect occurred when the rotating speed was equal to zero. The effect of surrounding temperature can be classified into two categories; cold working climate (low temperatures) and hot working climate (high temperatures).

The magnitudes of frequencies were raised under the cold climate conditions, because of the increment in the magnitude of the structural stiffness (elastic modulus). On the other hand, the magnitudes of frequencies were reduced under the warm/hot climate conditions. This occurred due to the decreasing of the values of the elastic modulus/structure stiffness. Furthermore, it can be concluded that the rotating blade stiffness was affected significantly by the speed of rotation and climate conditions, and this led to remarkable change in the magnitude of the stiffness of the structure. Also, it was found that the magnitudes of frequencies grew with the increasing of the blade's thickness owing to the increasing of the magnitudes of structural stiffness. The magnitudes of frequencies reduced once the thickness decreased, owing to the reducing in the magnitudes of structural stiffness.

The importance of this research paper lies in the study of the compound effect of rotational speed and thermal gradient on the rotating blades. The stiffness of the blade is variable and is a function of the speed of rotation and the ambient temperature. There are a few researchers who have studied such kind of problems. In the future researches, the same approach can be applied to investigate the thermal effect and rotation speed in addition to contact stresses of gear systems for example, or in tanks exposed to high temperatures and high pressure (fatigue stresses), etc. There are many problems in the engineering field that need this kind of careful analysis, which takes into account all the factors that directly affect the stiffness of structure/machine element and, as a result, its performance.

## REFERENCES

- [1] Farsadi, T. (2021). Enhancement of static and dynamic performance of composite tapered pretwisted rotating blade with variable stiffness. *Journal of Vibration and Acoustics*, 143 (2), 021009.
- [2] Ruan, Y., Hajek, M. (2021). Numerical investigation of dynamic stall on a single rotating blade. *Aerospace*, 8 (4), 90.
- [3] Chen, J., Li, Q.S. (2019). Vibration characteristics of a rotating pre-twisted composite laminated blade. *Composite Structures*, 208, 78-90.
- [4] Rafiee, M., Nitzsche, F., Labrosse, M. (2017). Dynamics, vibration and control of rotating composite beams and blades: A critical review. *Thin-Walled Structures*, 119, 795-819.
- [5] Yang, L., Mao, Z., Wu, S., Chen, X., Yan, R. (2021). Nonlinear dynamic behavior of rotating blade with breathing crack. *Frontiers of Mechanical Engineering*, 16 (1), 196-220.
- [6] Wang, D., Hao, Z., Chen, Y., Zhang, Y. (2018). Dynamic and resonance response analysis for a turbine blade with varying rotating speed. *Journal of Theoretical and Applied Mechanics*, 56 (1), 31-42.
- [7] Yao, M., Niu, Y., Hao, Y. (2019). Nonlinear dynamic responses of rotating pretwisted cylindrical shells. *Nonlinear Dynamics*, 95 (1), 151-174.
- [8] Ding, H., Zhu, M., Zhang, Z., Zhang, Y.W., Chen, L.Q. (2017). Free vibration of a rotating ring on an elastic foundation. *International Journal of Applied Mechanics*, 9 (4), 1750051.
- [9] Farsadi, T., Sener, O., Kayran, A. (2017). Free vibration analysis of uniform and asymmetric composite pretwisted rotating thin walled beam. In *ASME International Mechanical Engineering Congress and Exposition*. ASME, Vol. 58349.
- [10] Oh, S.Y., Song, O., Librescu, L. (2003). Effects of pretwist and presetting on coupled bending vibrations of rotating thin-walled composite beams. *International Journal of Solids and Structures*, 40 (5), 1203-1224.
- [11] Oh, Y., Yoo, H.H. (2016). Vibration analysis of rotating pretwisted tapered blades made of functionally graded materials. *International Journal of Mechanical Sciences*, 119, 68-79.
- [12] Yao, M.H., Ma, L., Zhang, M.M., Zhang, W. (2017). Vibration characteristics analysis of the rotating blade based on a polynomial aerodynamic force. In *International Design Engineering Technical Conferences and Computers and Information in Engineering Conference*. ASME, Vol. 58202.
- [13] Song, O., Librescu, L., Oh, S.Y. (2001). Vibration of pretwisted adaptive rotating blades modeled as anisotropic thin-walled beams. *AIAA Journal*, 39 (2), 285-295.
- [14] Xie, J., Liu, J., Chen, J., Zi, Y. (2022). Blade damage monitoring method base on frequency domain statistical index of shaft's random vibration. *Mechanical Systems and Signal Processing*, 165, 108351.
- [15] Xu, J., Qiao, B., Liu, M., Yang, Z., Chen, X. (2021). Crack propagation monitoring of rotor blades using synchroextracting transform. *Journal of Sound and Vibration*, 116253.

- [16] Zeng, J., Chen, K., Ma, H., Duan, T., Wen, B. (2019). Vibration response analysis of a cracked rotating compressor blade during run-up process. *Mechanical Systems and Signal Processing*, 118, 568-583.
- [17] Zienkiewicz, O.C., Taylor, R.L., Fox, D. (2005). *The Finite Element Method for Solid and Structural Mechanics*. Elsevier.
- [18] Ahmad, S., Irons, B.M., Zienkiewicz, O.C. (1970). Analysis of thick and thin shell structures by curved finite elements. *International Journal for Numerical Methods in Engineering*, 2 (3), 419-451.
- [19] Weaver, W., Johnston, P. (1987). *Structural Dynamic by Finite Elements*. Prentice-Hall.
- [20] Flower, G. (1996). Modeling of an elastic disc with finite hub motions and small elastic vibrations with application to rotor dynamics. *Journal of Vibration and Acoustics*, 118 (1), 10-15.
- [21] Henry, R., Lalanne M. (1974). Vibration analysis of rotating compressor blade. *Journal of Engineering for Industry*, 3, 1028-1035.
- [22] Cardarelli, F. (2018). *Materials Handbook*. Springer, 2254.
- [23] Carnegie, W. (1959). Vibrations of rotating cantilever blading: Theoretical approaches to the frequency problem based on energy methods. *Journal of Mechanical Engineering Science*, 1 (3), 235-240.

## Nomenclature

|                      |   |
|----------------------|---|
| $u$                  | Deflection in $x$ -direction [m]                  |
| $v$                  | Deflection in $y$ -direction [m]                  |
| $w$                  | Deflection in $z$ -direction [m]                  |
| $\alpha$             | rotations around $X'$ axis [rad]                  |
| $\beta$              | rotations around $Y'$ axis [rad]                  |
| $\varepsilon_x$      | Strain in $x$ -direction                          |
| $\varepsilon_y$      | Strain in $y$ -direction                          |
| $\varepsilon_z$      | Strain in $z$ -direction                          |
| $[B]$                | Strain-Displacement matrix                        |
| $[K]$                | Stiffness matrix                                  |
| $[D]$                | Stress-Strain matrix                              |
| $[M]$                | Mass matrix                                       |
| $[N]$                | Shape function matrix                             |
| $K_G$                | Stiffness of the initial stresses                 |
| $\vec{F}$            | Forces load vector                                |
| $E$                  | Young's modulus of elasticity [N/m <sup>2</sup> ] |
| $\theta$             | Torsional displacement [rad]                      |
| $\zeta, \eta, \zeta$ | Natural curvilinear coordinates                   |
| $\rho$               | Mass density [kg/m <sup>3</sup> ]                 |
| $\nu$                | Poisson's ratio                                   |
| $T$                  | Temperature of working environment [°C]           |

Received December 16, 2021

Accepted February 07, 2022